

Chloride Oxidation by One- or Two-Photon Excitation of *N*-Phenylphenothiazine

Pengju Li, Alexander M. Deetz, Jiaming Hu, Gerald J. Meyer,* and Ke Hu*



Cite This: *J. Am. Chem. Soc.* 2022, 144, 17604–17610



Read Online

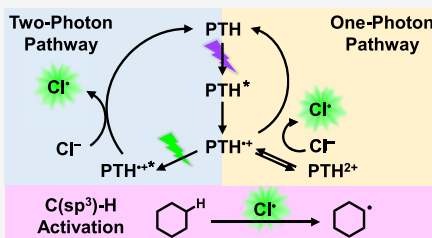
ACCESS |

Metrics & More

Article Recommendations

Supporting Information

ABSTRACT: Chloride oxidation has tremendous utility in the burgeoning field of chlorine-mediated C–H activation, yet it remains a challenging process to initiate with light because of the exceedingly positive one-electron reduction potential, E° ($\text{Cl}^{\bullet-}$), beyond most common transition-metal photooxidants. Herein, two photocatalytic chloride oxidation pathways that involve either one- or consecutive two-photon excitation of *N*-phenylphenothiazine (PTH) are presented. The one-photon pathway generates $\text{PTH}^{\bullet+}$ by oxidative quenching that subsequently disproportionates to yield PTH^{2+} that oxidizes chloride; this pathway is also accessed by the electrochemical oxidation of PTH. The two-photon pathway, which proceeded through the radical cation excited state, $^2\text{PTH}^{\bullet+\bullet}$, was of particular interest as this super-photooxidant was capable of directly oxidizing chloride to chlorine atoms. Laser flash photolysis revealed that the photooxidation by the doublet excited state proceeded on a subnanosecond timescale through a static quenching mechanism with an ion-pairing equilibrium constant of 0.36 M^{-1} . The PTH photoredox chemistry was quantified spectroscopically on nanosecond and longer time scales, and chloride oxidation chemistry was revealed by reactivity studies with model organic substrates. One- and two-photon excitation of PTH enabled chlorination of unactivated $\text{C}(\text{sp}^3)$ –H bonds of organic compounds such as cyclohexane with substantial yield enhancement observed from inclusion of the second excitation wavelength. This study provides new mechanistic insights into chloride oxidation catalyzed by an inexpensive and commercially available organic photooxidant.



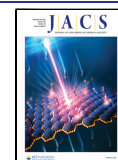
INTRODUCTION

Chlorine atoms have long been known as a powerful tool for C–H activation yet historically have seen little use in practical applications due to the harsh reaction conditions necessary to generate Cl^\bullet . Over the last decade, a number of groundbreaking studies have demonstrated facile chloride oxidation using photoredox catalysts, which have enabled new approaches to functionalize inert C–H bonds.^{1–12} Additionally, environmentally motivated applications rely on chloride oxidation as an important fundamental process for HCl splitting to store solar energy^{13–15} or for electric gradient generation for sea water desalination.^{16–19} However, the vast majority of these examples rely on noble metal photocatalysts to generate chlorine atoms because the one-electron reduction potential, $(\text{Cl}^{\bullet-})$, requires an incredibly potent photooxidant.^{20–22} Indeed, chloride ions are so redox inert that they are frequently used as counterions for common photocatalysts such as ruthenium polypyridyl compounds.^{23,24} Synthesizing ruthenium or iridium coordination compounds that are strong photooxidants requires skillful ligand engineering^{1,25–28} and such catalysts often suffer from stability issues.^{29–31} Moreover, photocatalysts based on noble metals are impractical at scale given the low natural abundance of these rare elements. Herein, we report a rare example of light-induced chloride oxidation catalyzed by an inexpensive, commercially available organic photocatalyst through unconventional one- and two-photon pathways.

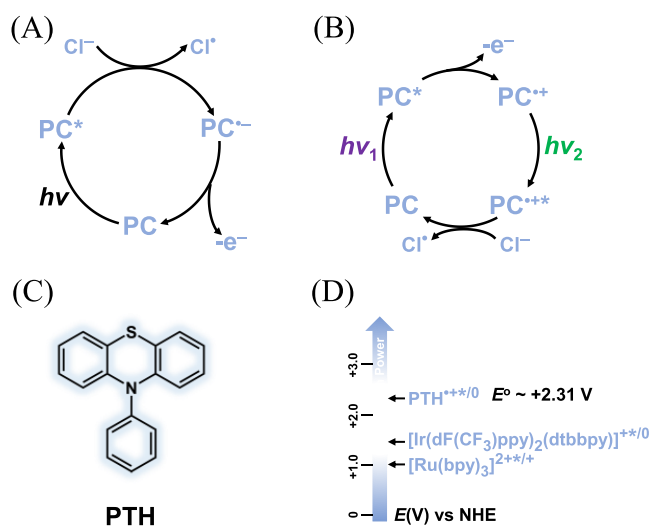
In recent years, molecular doublet excited states of organic photocatalysts, which can be generated from consecutive light excitation, have been used to great avail as potent photo-reductants in photoredox catalysis;^{32–37} however, their use as photooxidants remains relatively rare.^{38–41} Phenothiazine and its derivatives are one of the few radical cations studied for their oxidizing excited state properties.^{42,43} In this study, we show that two-photon excitation of *N*-phenylphenothiazine (PTH) generates the highly oxidizing doublet excited state, $^2\text{PTH}^{\bullet+\bullet}$, which catalyzes the energy-demanding oxidation of chloride to the chlorine atom (Scheme 1). Two-color two-pulse laser flash photolysis demonstrated the rapid subnanosecond electron transfer process. Our results also suggest a second, albeit less efficient, mechanism of chloride oxidation occurs in competition with the two-photon pathway. Activation of $\text{C}(\text{sp}^3)$ –H bonds in a series of substrates was achieved by steady-state illumination of PTH, demonstrating the potential utility of this approach to synthetic chemistry applications.

Received: July 6, 2022

Published: September 14, 2022

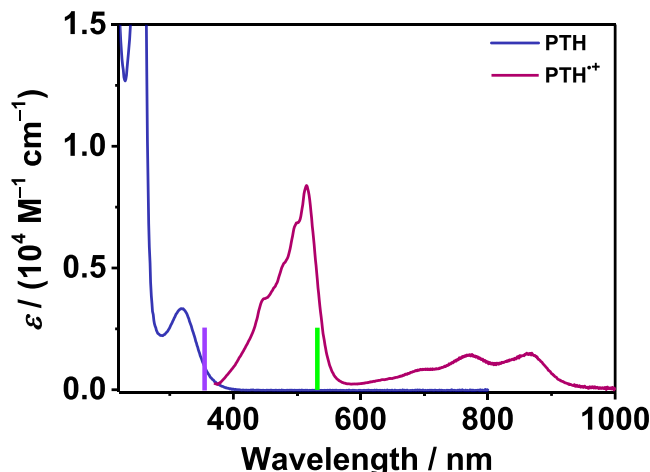


Scheme 1. Conventional Photoredox (A) and Two-Photon (B) Mechanisms for Halide Oxidation and Excited-State Reduction Potentials for Prototypical Photocatalysts (C,D)



RESULTS

The absorbance spectrum of PTH in CH₃CN displayed UV bands characteristic of $\pi \rightarrow \pi^*$ transitions at 255 and 320 nm (Figure 1). Strong room temperature fluorescence centered



around 450 nm decayed with a lifetime of 3.0 ns, Figure S1, which was in good agreement with previously published data.⁴⁴ Cyclic voltammetry experiments showed a reversible PTH oxidation of $E^\circ(\text{PTH}^{\bullet+/0}) = 0.92$ V vs NHE and a second irreversible oxidation for (PTH^{2+/•+}) at 1.59 V vs NHE (estimated from the half anodic peak height) in CH₃CN electrolyte solutions (Figure S2). Spectroelectrochemistry measurements revealed that as the potential bias was increased from 0 to 1.13 V vs NHE, new absorption features assigned to PTH^{•+} were observed at 514, 772, and 864 nm, with concomitant loss of the ground-state absorbance. The spectroelectrochemical data were fully consistent with the absorbance of PTH^{•+} obtained from chemical oxidation by Cu(ClO₄)₂. The energy stored in the excited state ($E_{0,0}$) for

PTH^{•+}* was extracted from the intersection of the absorption spectrum and previously reported photoluminescence,⁴³ $E_{0,0} = 1.39$ eV. The excited state redox potential for the doublet excited state PTH^{•+}* was then approximated using the equation $E^\circ(\text{PTH}^{\bullet+/0}) = E^\circ(\text{PTH}^{\bullet+/0}) + E_{0,0} = 2.31$ V vs NHE.

Transient absorption (TA) spectra were collected following pulsed-laser excitation ($\lambda_{\text{ex}} = 355$ nm) of PTH dissolved in argon-purged and aerated CH₃CN (Figure 2A and B,

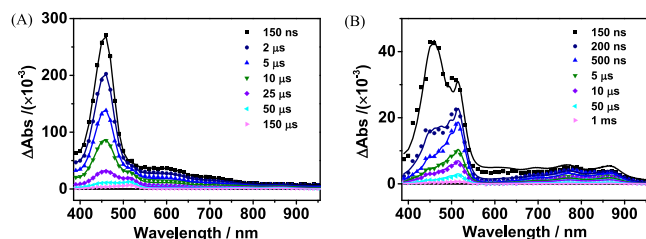


Figure 2. Absorption difference spectra of PTH in argon-purged CH₃CN (A) or aerated CH₃CN (B) after pulsed laser excitation ($\lambda_{\text{ex}} = 355$ nm) at the indicated delay times. Overlaid solid curves on the transient spectra at each delay time are the simulations based on linear combinations of the ³PTH* spectrum obtained from (A) and the PTH^{•+} spectrum obtained from spectroelectrochemistry.

respectively). The argon-saturated spectra displayed a strong feature at 460 nm assigned to absorbance of ³PTH* based on the previously reported triplet excited state of the parent phenothiazine (PTZ) complex.⁴⁵ In aerated CH₃CN, the TA spectra recorded at short time delays showed a similar absorbance at 460 nm with an additional absorbance feature centered at 510 nm. By 500 ns, the feature at 460 nm fully decayed and only the absorbance at 510 nm remained; spectra at time delays ≥ 500 ns were fully normalizable—indicative of only one state—and were fully consistent with the PTH^{•+} absorption spectrum obtained from spectroelectrochemistry. Formation of PTH^{•+} was only observed in aerated PTH solutions, indicating that dioxygen served as an electron acceptor. It should be noted that at long time delays in the argon-saturated spectrum, a small shoulder at 510 nm became more evident, attributed to PTH ionization forming PTH^{•+} and a solvated electron, as was previously reported for PTZ.⁴² Because the presence of ³PTH* introduced additional spectral complexities that were not of primary interest to the present study, all subsequent kinetic studies unless otherwise specified were performed under oxygen-saturated environments, where ³PTH* was nearly quenched on the nanosecond time scale.

The TA spectra recorded in the presence of chloride showed the same absorbance features as were observed in the absence of chloride (Figure S3). However, single wavelength kinetics monitored at 510 nm indicated that PTH^{•+} absorbance decayed more slowly in the presence of the first aliquot of TBACl. A similar behavior was observed with the addition of TBAClO₄, albeit to a lesser extent, suggesting that an increased ionic strength retards recombination, although the precise origin of this behavior is not fully understood. Interestingly, additional aliquots of chloride led to a decrease in PTH^{•+} lifetime with a first-order concentration dependence in the chloride concentration, indicating a new PTH^{•+} redox reaction in the presence of chloride.

¹H NMR was used to probe whether net chemistry occurred between TBACl with PTH^{•+}. Chemical oxidation of PTH was

performed by stoichiometric addition of $\text{Cu}(\text{ClO}_4)_2$, which resulted in the disappearance of all the aromatic hydrogen resonances. Subsequent addition of excess TBACl to the NMR sample led to complete regeneration of the hydrogen signals corresponding to PTH (Figure S4). While this would ostensibly indicate reduction of PTH^{*+} by chloride, the one-electron potential for $E^\circ(\text{Cl}^{*-})$ in CH_3CN has been crudely estimated as 1.46 V vs NHE;^{20,27} therefore, reduction of PTH^{*+} by chloride is strongly thermodynamically disfavored.

Cyclic voltammetry experiments where tetrabutylammonium chloride (TBACl) was titrated into a solution of PTH led to a progressively less reversible $\text{PTH}^{*+/0}$ redox couple, indicated by complete loss of the cathodic reduction return feature in the presence of 60 mM TBACl (~3 equiv) (Figure 3).

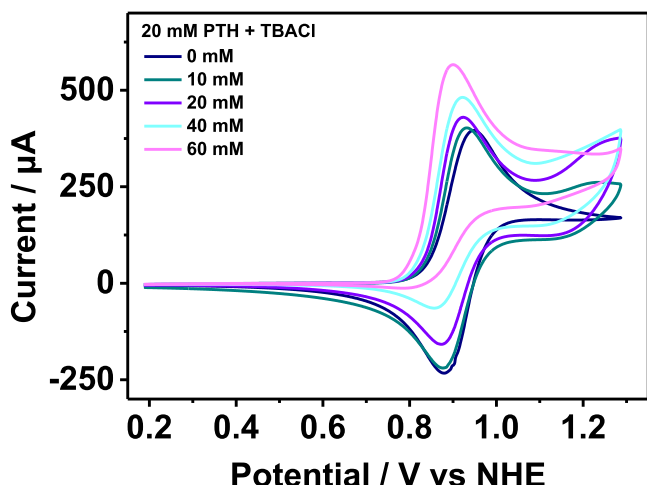


Figure 3. Cyclic voltammograms of PTH in 0.1 M TBAClO_4 CH_3CN with the indicated TBACl concentrations.

Interestingly, increasing the chloride concentration led to an increase in the anodic current, consistent with a catalytic reaction mechanism in which chloride regenerates PTH^0 . Given the reduction potentials of the species involved, an endergonic reaction between PTH^{*+} and Cl^- seems highly unlikely. Indeed, similar voltammetry experiments in which PTH was replaced by $[\text{Ir}(\text{ppy})_3]$, where ppy is phenylpyridine, showed no evidence for chloride oxidation, even though it has a more positive reduction potential, $E^\circ(\text{Ir}^{\text{IV}/\text{III}}) = 0.95$ V vs NHE (Figure S2D). Taken together, the most compelling explanation is a previously postulated disproportionation reaction,⁴⁶ $2\text{PTH}^{*+} \rightleftharpoons \text{PTH} + \text{PTH}^{2+}$, where PTH^{2+} is capable of thermally oxidizing chloride in CH_3CN . Because the first reversible oxidation of $\text{PTH}^{*+/0}$ precedes the second irreversible $\text{PTH}^{2+/*+}$ oxidation, the disproportionation equilibrium strongly favors PTH^{*+} . However, chloride oxidation shifts the equilibrium toward the direction of disproportionation. A kinetic model for the disproportionation reactivity observed in the presence of chloride was derived and shown in the Supporting Information. Fitting the TA kinetics to this model provided a disproportionation equilibrium constant of $5.5 \times 10^{-8} \text{ M}^{-1}$ (Figure S5).

A two-photon, two-color excitation pulse sequence was used to generate ${}^2\text{PTH}^{*+*}$, as indicated in the Figure 4A inset. The first laser pulse at 355 nm generated the long-lived PTH^{*+} from PTH^* as described above. The second pulse at 532 nm was delayed by 500 ns relative to the first pulse to generate ${}^2\text{PTH}^{*+*}$ from the transiently generated PTH^{*+} . Figure 4A

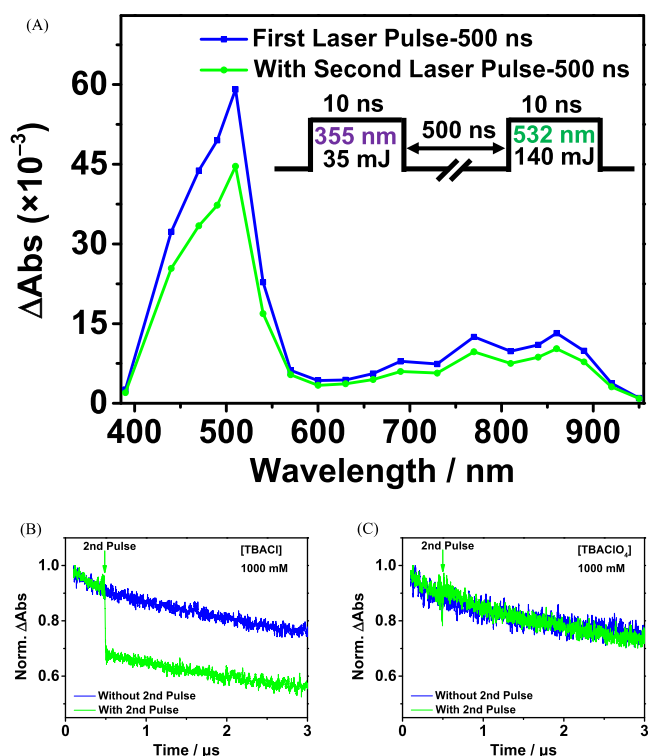


Figure 4. (A) Absorption difference spectra of PTH in the presence of 1000 mM TBACl in a two-pulse experiment with a pre-second pulse spectrum shown in blue and a post-second pulse spectrum shown in green (inset: the two-pulse sequence). Transient kinetic data for the oxidized PTH monitored at the probe wavelength of 510 nm in a two-pulse experiment with (B) 1000 mM TBACl or (C) 1000 mM TBAClO_4 in the CH_3CN solution. Traces in blue are without the second laser pulse excitation and the traces in green are with the second laser pulse delayed by 500 ns after the first laser pulse.

shows the TA spectra of PTH in the presence of 1000 mM TBACl immediately before and after the second laser pulse, where the transient absorbance at a given wavelength are denoted as $\Delta\text{Abs}_{\text{PP}}$ (pump-probe) and $\Delta\text{Abs}_{\text{PPP}}$ (pump-pump-probe), respectively. The second laser pulse did not generate any new absorbance features, but a substantial bleach of the PTH^{*+} absorption was observed (Figure 4B). Kinetics monitored at 510 nm showed that titration of TBACl ranging from concentrations of 100 to 1000 mM resulted in progressively larger bleaches directly following the second pulse (Figure S6). A control experiment where TBACl additions were replaced by the redox inert TBAClO_4 exhibited negligible change in absorbance upon the second laser pulse (Figure 4C). The ratio of $\Delta\text{Abs}_{\text{PP}}/\Delta\text{Abs}_{\text{PPP}}$ versus TBACl yielded a linear Stern–Volmer type plot, indicating a reaction that was first order in chloride concentration with a slope of $K_S = 0.36 \text{ M}^{-1}$ (Figure 5).

Steady-state photolysis of PTH and TBACl was performed in the presence of a halogen atom trap, 1,1-diphenylethene (DPE).^{47,48} Continuous irradiation with 390 and 532 nm light through two sides of the sample yielded the photoproduct where one chlorine atom was added to DPE, identified by gas chromatography–mass spectrometry (GC–MS) (Figure S7). Control experiments indicated that irradiation with exclusively 390 nm light generated some chlorine-substituted DPE but with a significantly diminished yield, which is consistent with trace chlorine-atom formation from the aforementioned

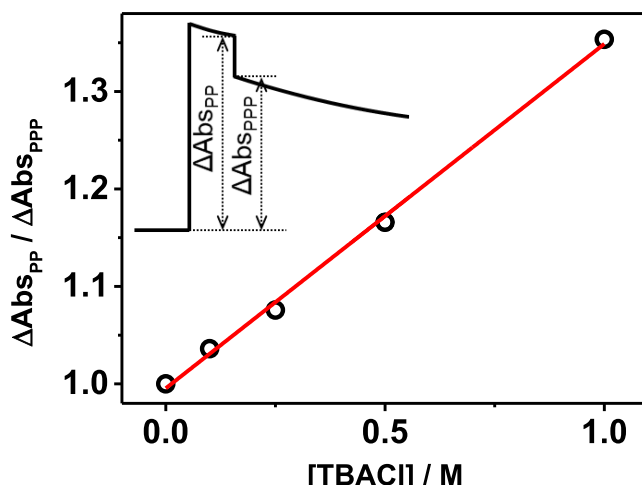
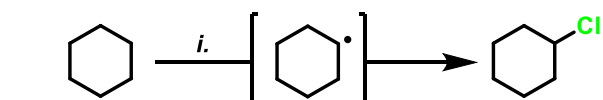


Figure 5. Stern–Volmer plot based on the two-pulse experiment upon titration of TBACl. The subscripts PP stands for pump-probe and PPP stands for pump-pump-probe. Inset: schematic illustration of the two quantities $\Delta\text{Abs}_{\text{PP}}$ and $\Delta\text{Abs}_{\text{PPP}}$. See text for further details.

disproportionation mechanism. Addition of TBACl and DPE to electrochemically generated PTH^{*+} under stoichiometric conditions also led to the formation of chlorine-substituted DPE, providing further evidence for disproportionation reactivity even in the absence of light. Additional controls demonstrated that all three chemical components—PTH, DPE, and TBACl—were necessary to detect the chlorinated photoproduct. While the multiple chloride oxidation mechanisms are of fundamental interest, it is important to note that the yield of chlorine-substituted DPE was 85% higher under two-color illumination.

Successful chlorine-atom trapping experiments inspired us to determine whether one- and two-photon excitation of PTH could enable reactivity with unactivated $\text{C}(\text{sp}^3)-\text{H}$ bonds using cyclohexane as a model substrate. Photolysis results from other substrates including toluene, 1,4-dioxane, and cycloheptane that represent good structural diversity are also shown in the Supporting Information (Figure S8). Initial trials conducted under identical conditions as the previously described steady-state photolysis experiments yielded C–H activation products where oxygenation of the cyclohexane was observed due to the reaction of the transient carbon radical (Figure 6) with dioxygen, as has been previously observed.⁵ Replacing dioxygen with CCl_4 as the sacrificial electron acceptor enabled generation of the chlorinated C–H activation photoproduct, chlorocyclohexane.⁴⁹ (Note that 405 nm light was used in place of 390 nm to avoid direct excitation of CCl_4 .) Consistent with our other steady-state photolysis experiments, inclusion of the second light source at 532 nm that exclusively excited PTH^{*+} resulted in 38% increase of the chlorination product (Figure 6). The proposed mechanism for halogenation of cyclohexane starts with hydrogen atom abstraction by the photogenerated chlorine atom in which HCl and cyclohexane radicals were the secondary photo-products. The final chlorocyclohexane product was obtained by cyclohexane radical either abstracting a chlorine atom from CCl_4 or capturing another photogenerated chlorine atom in the solution. It should be noted that the actual chlorine atom source could also be from Cl_2^{*+} or Cl_3^- due to multiple equilibria among chlorine species in the presence of excess chloride.²²



i. PTH (2 mol%), CCl_4 (200 mM), TBACl (100 mM), CH_3CN , Ar, r.t., 405 nm and 532 nm, 40 min

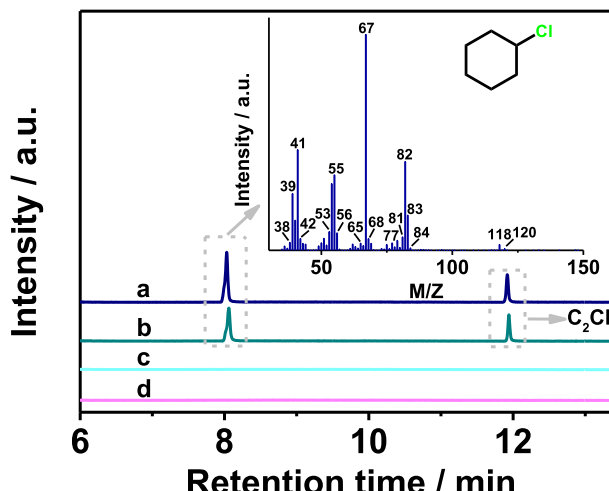


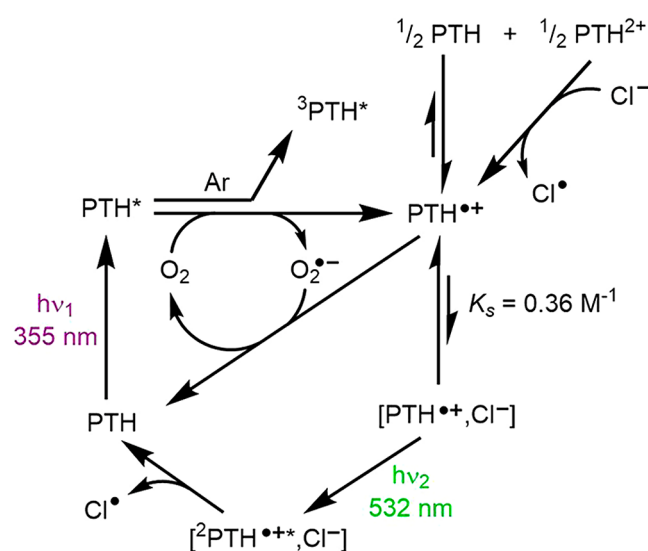
Figure 6. GC–MS analysis of the photocatalytic chlorination reaction of an unactivated $\text{C}(\text{sp}^3)-\text{H}$ bond on cyclohexane. (a) PTH + CCl_4 + TBACl + cyclohexane + 405 and 532 nm irradiation, (b) PTH + CCl_4 + TBACl + cyclohexane + 405 nm irradiation, (c) PTH + TBACl + cyclohexane + 405 nm irradiation, and (d) CCl_4 + TBACl + cyclohexane + 405 nm irradiation. (PTH: 20 mM, CCl_4 : 200 mM, TBACl: 100 mM, Cyclohexane: 1 M in CH_3CN , Ar, r.t., 405 nm: 100 mW, 532 nm: 1.3 W, 40 min). Inset shows the mass spectrum for the photoproduct detected at the retention time of 8.06 min.

DISCUSSION

The electrochemical, spectroscopic, and reactivity studies reported herein provide compelling evidence for a two-photon technique to generate chlorine atoms in oxygenated solutions. The first photon, $h\nu_1$, creates the oxidized donor PTH^{*+} and the second photon, $h\nu_2$, selectively excites PTH^{*+} to generate a super-photooxidant $^2\text{PTH}^{*+*}$ that oxidizes chloride on a sub-10 ns time scale. The complete proposed mechanism is shown in Scheme 2. Interestingly, there was clear evidence for some chloride oxidation in the absence of the second photon and when PTH^{*+} was generated electrochemically. Below, we discuss this PTH^{*+} reactivity followed by a more detailed analysis of the two-photon mechanism.

The lifetime of the photogenerated PTH^{*+} decreased when the chloride concentration was increased from 100 to 1000 mM. Direct chloride oxidation by PTH^{*+} is thermodynamically uphill by >500 mV and hence an unlikely pathway. Early studies on phenothiazine radical cations suggested that chloride may substitute the aromatic hydrogen atoms through nucleophilic attack;⁵⁰ however, ^1H NMR analysis reported here revealed no evidence for net photochemistry. Instead, a more likely disproportionation mechanism is proposed that generates the two-electron oxidized donor, $2\text{PTH}^{*+} \rightleftharpoons \text{PTH} + \text{PTH}^{2+}$.⁴⁶ The PTH^{2+} is a potent oxidant competent of generating chlorine atoms that reacted with the olefin trap 1,1-diphenylethene. Hence, light-initiated or electrochemical generation of PTH^{*+} resulted in chloride oxidation, although the two-photon approach described below results in a markedly higher yield.

Scheme 2. Proposed Mechanism of Chloride Oxidation by Multiple PTH-Mediated Pathways



Green light excitation of $\text{PTH}^{•+}$ formed the extremely potent photooxidant ${}^2\text{PTH}^{•+*}$ with an excited state reduction potential >2.3 V vs NHE. The excited state lifetime of ${}^2\text{PTH}^{•+*}$ was previously reported to be 36 ps,⁴³ which precludes dynamic (diffusional) quenching at the concentrations utilized. Fortunately, this cation forms a weak ion pair with chloride, $K_s = 0.36 \text{ M}^{-1}$, in CH_3CN that rapidly reacts without diffusional limitations, $k_{\text{et}} > 10^8 \text{ s}^{-1}$, to regenerate the PTH ground state. While the spectroscopic data provided compelling evidence of reductive electron transfer and ${}^2\text{PTH}^{•+*} \rightarrow \text{PTH}$ conversion, the chloride oxidation products were not observed spectroscopically. Previous pulse radiolysis studies have indicated that aqueous chloride oxidation yields the chlorine atom (Cl^{\cdot}) and the dichloride radical anion ($\text{Cl}_2^{\cdot-}$).^{51,52} Both products are expected due to the $\text{Cl}^{\cdot} + \text{Cl} \rightleftharpoons \text{Cl}_2^{\cdot-}$ equilibrium. For simplicity, only the chlorine atom is shown in Scheme 2, but a similar equilibrium is expected in CH_3CN . In any event, both of these oxidized species absorb weakly in the ultraviolet region and were not detected following two-photon excitation.

Direct evidence for the presence of oxidized chloride species was provided by reactivity studies first with a halogen atom trap, 1,1-diphenylethene (DPE), and then with substrates containing unactivated $\text{C}(\text{sp}^3)-\text{H}$ bonds. Chlorine-substituted DPE was observable from the reaction of TBACl with electrochemically generated $\text{PTH}^{•+}$ by the aforementioned disproportionation pathway. Illumination of PTH with only blue light generated some chlorinated photoproduct, which was also attributed to reactivity enabled by disproportionation. An additional possibility is that while the blue light absorbance of $\text{PTH}^{•+}$ is small, prior research has reported excitation at 390 nm to form $\text{PTH}^{•+*}$, although undoubtably with lower efficiency than 532 nm.³⁸ Addition of the green light source to photolysis experiments ensured generation of ${}^2\text{PTH}^{•+*}$, which enabled the two-photon pathway in Scheme 2. Two-photon illumination resulted in chlorinated photoproduct yields that were enhanced by 85 and 38% for DPE and cyclohexane, respectively, relative to single-wavelength illumination. The generality of this approach was established using the additional substrates toluene, 1,4-dioxane, and cyclo-

heptane, which resulted in analogous C–H activation and chlorination in two-photon photolysis experiments. Reactivity studies demonstrating chlorination of vinylic, benzylic, α -alkoxy, and unactivated aliphatic C–H bonds, coupled with time-resolved absorption studies, provided compelling evidence that ${}^2\text{PTH}^{•+*}$ was reductively quenched by chloride to form the chlorine atom intermediate as the primary photoproduct.

CONCLUSIONS

In conclusion, the organic photocatalyst PTH was shown to photo-oxidize chloride in CH_3CN solutions. Two photocatalytic pathways that generate potent oxidants, PTH^{2+} or ${}^2\text{PTH}^{•+*}$, were identified. The former was generated by one-photon excitation of PTH followed by disproportionation, whereas the latter ${}^2\text{PTH}^{•+*}$ was formed by a consecutive two-photon excitation pathway. Mechanistic studies based on two-pulse two-color laser flash photolysis experiments revealed that chloride photo-oxidation occurred on a subnanosecond time scale through an ion pair at high chloride concentrations. While transient kinetic studies were based on a timed sequence of two laser pulses, this photoredox chemistry was also shown to be operative with two steady-state light sources through the activation of $\text{C}(\text{sp}^3)-\text{H}$ bonds for accelerated synthesis of a variety of chlorinated organic compounds. The two-photon approach to chloride oxidation is a more desirable option for synthetic and environmental applications because of the panchromatic light absorption by the oxidized PTH to yield ${}^2\text{PTH}^{•+*}$ as a super-photooxidant. The study demonstrates that the generation of a potent organic radical cation excited state enables rapid chloride oxidation to the highly reactive and synthetically useful chlorine atom intermediate.

ASSOCIATED CONTENT

Supporting Information

The Supporting Information is available free of charge at <https://pubs.acs.org/doi/10.1021/jacs.2c07107>.

Experimental details; additional spectroscopic and electrochemical characterizations; kinetic model derivation; and GC–MS product analysis for photolysis (PDF)

AUTHOR INFORMATION

Corresponding Authors

Gerald J. Meyer – Department of Chemistry, University of North Carolina at Chapel Hill, Chapel Hill, North Carolina 27599-3290, United States; orcid.org/0000-0002-4227-6393; Email: gjmeyer@email.unc.edu

Ke Hu – Department of Chemistry and Shanghai Key Laboratory of Molecular Catalysis and Innovative Materials, Fudan University, Shanghai 200433, P. R. China; orcid.org/0000-0002-0240-7192; Email: khu@fudan.edu.cn

Authors

Pengju Li – Department of Chemistry and Shanghai Key Laboratory of Molecular Catalysis and Innovative Materials, Fudan University, Shanghai 200433, P. R. China

Alexander M. Deetz – Department of Chemistry, University of North Carolina at Chapel Hill, Chapel Hill, North Carolina 27599-3290, United States

Jiaming Hu — Department of Materials Science, Fudan University, Shanghai 200433, P. R. China

Complete contact information is available at:
<https://pubs.acs.org/10.1021/jacs.2c07107>

Notes

The authors declare no competing financial interest.

ACKNOWLEDGMENTS

P.L., J.H., and K.H. acknowledge the funding support from the National Natural Science Foundation of China (22173022) and the Natural Science Foundation of Shanghai (21ZR1404400). A.M.D. and G.J.M. acknowledge the National Science Foundation under Award CHE-1465060 for research funding. A.M.D. additionally acknowledges the Department of Chemistry at the University of North Carolina for providing individual funding through the Eliel Fellowship.

REFERENCES

- (1) Rohe, S.; Morris, A. O.; McCallum, T.; Barriault, L. Hydrogen Atom Transfer Reactions via Photoredox Catalyzed Chlorine Atom Generation. *Angew. Chem., Int. Ed.* **2018**, *57*, 15664–15669.
- (2) Xu, P.; Chen, P.-Y.; Xu, H.-C. Scalable Photoelectrochemical Dehydrogenative Cross-Coupling of Heteroarenes with Aliphatic C–H Bonds. *Angew. Chem., Int. Ed.* **2020**, *59*, 14275–14280.
- (3) Deng, H.-P.; Zhou, Q.; Wu, J. Microtubing-Reactor-Assisted Aliphatic C–H Functionalization with HCl as a Hydrogen-Atom-Transfer Catalyst Precursor in Conjunction with an Organic Photoredox Catalyst. *Angew. Chem., Int. Ed.* **2018**, *57*, 12661–12665.
- (4) Panetti, G. B.; Yang, Q.; Gau, M. R.; Carroll, P. J.; Walsh, P. J.; Schelter, E. J. Discovery and mechanistic investigation of photo-induced sp³ C–H activation of hydrocarbons by the simple anion hexachlorotitanate. *Chem. Catal.* **2022**, *2*, 853–866.
- (5) Ohkubo, K.; Fujimoto, A.; Fukuzumi, S. Metal-free oxygenation of cyclohexane with oxygen catalyzed by 9-mesityl-10-methylacridinium and hydrogen chloride under visible light irradiation. *Chem. Commun.* **2011**, *47*, 8515–8517.
- (6) Zidan, M.; Morris, A. O.; McCallum, T.; Barriault, L. The Alkylation and Reduction of Heteroarenes with Alcohols Using Photoredox Catalyzed Hydrogen Atom Transfer via Chlorine Atom Generation. *Eur. J. Org. Chem.* **2020**, *2020*, 1453–1458.
- (7) Gonzalez, M. I.; Gygi, D.; Qin, Y.; Zhu, Q.; Johnson, E. J.; Chen, Y.-S.; Nocera, D. G. Taming the Chlorine Radical: Enforcing Steric Control over Chlorine-Radical-Mediated C–H Activation. *J. Am. Chem. Soc.* **2022**, *144*, 1464–1472.
- (8) Gygi, D.; Gonzalez, M. I.; Hwang, S. J.; Xia, K. T.; Qin, Y.; Johnson, E. J.; Gygi, F.; Chen, Y.-S.; Nocera, D. G. Capturing the Complete Reaction Profile of a C–H Bond Activation. *J. Am. Chem. Soc.* **2021**, *143*, 6060–6064.
- (9) Hirscher, N. A.; Ohri, N.; Yang, Q.; Zhou, J.; Anna, J. M.; Schelter, E. J.; Goldberg, K. I. A Metal-Free, Photocatalytic Method for Aerobic Alkane Iodination. *J. Am. Chem. Soc.* **2021**, *143*, 19262–19267.
- (10) Shields, B. J.; Doyle, A. G. Direct C(sp³)–H Cross Coupling Enabled by Catalytic Generation of Chlorine Radicals. *J. Am. Chem. Soc.* **2016**, *138*, 12719–12722.
- (11) Wang, Y.-H.; Yang, Q.; Walsh, P. J.; Schelter, E. J. Light-mediated aerobic oxidation of C(sp³)–H bonds by a Ce(IV) hexachloride complex. *Org. Chem. Front.* **2022**, *9*, 2612–2620.
- (12) Yang, Q.; Wang, Y.-H.; Qiao, Y.; Gau, M.; Carroll, P. J.; Walsh, P. J.; Schelter, E. J. Photocatalytic C–H activation and the subtle role of chlorine radical complexation in reactivity. *Science* **2021**, *372*, 847–852.
- (13) McDaniel, N. D.; Bernhard, S. Solar fuels: thermodynamics, candidates, tactics, and figures of merit. *Dalton Trans.* **2010**, *39*, 10021–10030.
- (14) Li, Z.; Luo, L.; Li, M.; Chen, W.; Liu, Y.; Yang, J.; Xu, S.-M.; Zhou, H.; Ma, L.; Xu, M.; Kong, X.; Duan, H. Photoelectrocatalytic C–H halogenation over an oxygen vacancy-rich TiO₂ photoanode. *Nat. Commun.* **2021**, *12*, 6698.
- (15) Powers, D. C.; Anderson, B. L.; Nocera, D. G. Two-Electron HCl to H₂ Photocycle Promoted by Ni(II) Polypyridyl Halide Complexes. *J. Am. Chem. Soc.* **2013**, *135*, 18876–18883.
- (16) Kim, B.-J.; Piao, G.; Kim, S.; Yang, S. Y.; Park, Y.; Han, D. S.; Shon, H. K.; Hoffmann, M. R.; Park, H. High-Efficiency Solar Desalination Accompanying Electrocatalytic Conversions of Desalinated Chloride and Captured Carbon Dioxide. *ACS Sustainable Chem. Eng.* **2019**, *7*, 15320–15328.
- (17) Kim, S.; Han, D. S.; Park, H. Reduced titania nanorods and Ni–Mo–S catalysts for photoelectrocatalytic water treatment and hydrogen production coupled with desalination. *Appl. Catal. B Environ.* **2021**, *284*, No. 119745.
- (18) Kim, S.; Piao, G.; Han, D. S.; Shon, H. K.; Park, H. Solar desalination coupled with water remediation and molecular hydrogen production: a novel solar water-energy nexus. *Energy Environ. Sci.* **2018**, *11*, 344–353.
- (19) Knust, K. N.; Hlushko, D.; Anand, R. K.; Tallarek, U.; Crooks, R. M. Electrochemically Mediated Seawater Desalination. *Angew. Chem., Int. Ed.* **2013**, *52*, 8107–8110.
- (20) Deetz, A. M.; Troian-Gautier, L.; Wehlin, S. A. M.; Piechota, E. J.; Meyer, G. J. On the Determination of Halogen Atom Reduction Potentials with Photoredox Catalysts. *J. Phys. Chem. A* **2021**, *125*, 9355–9367.
- (21) Isse, A. A.; Lin, C. Y.; Coote, M. L.; Gennaro, A. Estimation of Standard Reduction Potentials of Halogen Atoms and Alkyl Halides. *J. Phys. Chem. B* **2011**, *115*, 678–684.
- (22) Troian-Gautier, L.; Turlington, M. D.; Wehlin, S. A. M.; Maurer, A. B.; Brady, M. D.; Swords, W. B.; Meyer, G. J. Halide Photoredox Chemistry. *Chem. Rev.* **2019**, *119*, 4628–4683.
- (23) Ward, W. M.; Farnum, B. H.; Siegler, M.; Meyer, G. J. Chloride Ion-Pairing with Ru(II) Polypyridyl Compounds in Dichloromethane. *J. Phys. Chem. A* **2013**, *117*, 8883–8894.
- (24) Troian-Gautier, L.; Beauvilliers, E. E.; Swords, W. B.; Meyer, G. J. Redox Active Ion-Paired Excited States Undergo Dynamic Electron Transfer. *J. Am. Chem. Soc.* **2016**, *138*, 16815–16826.
- (25) Wehlin, S. A. M.; Troian-Gautier, L.; Li, G.; Meyer, G. J. Chloride Oxidation by Ruthenium Excited-States in Solution. *J. Am. Chem. Soc.* **2017**, *139*, 12903–12906.
- (26) Brady, M. D.; Sampaio, R. N.; Wang, D.; Meyer, T. J.; Meyer, G. J. Dye-Sensitized Hydrobromic Acid Splitting for Hydrogen Solar Fuel Production. *J. Am. Chem. Soc.* **2017**, *139*, 15612–15615.
- (27) Bevernaeghe, R.; Wehlin, S. A. M.; Piechota, E. J.; Abraham, M.; Philouze, C.; Meyer, G. J.; Elias, B.; Troian-Gautier, L. Improved Visible Light Absorption of Potent Iridium(III) Photo-oxidants for Excited-State Electron Transfer Chemistry. *J. Am. Chem. Soc.* **2020**, *142*, 2732–2737.
- (28) Deetz, A. M.; Meyer, G. J. Resolving Halide Ion Stabilization through Kinetically Competitive Electron Transfers. *JACS Au* **2022**, *2*, 985–995.
- (29) Li, G.; Brady, M. D.; Meyer, G. J. Visible Light Driven Bromide Oxidation and Ligand Substitution Photochemistry of a Ru Diimine Complex. *J. Am. Chem. Soc.* **2018**, *140*, 5447–5456.
- (30) White, J. K.; Schmehl, R. H.; Turro, C. An overview of photosubstitution reactions of Ru(II) imine complexes and their application in photobiology and photodynamic therapy. *Inorg. Chim. Acta* **2017**, *454*, 7–20.
- (31) Luis, E. T.; Iranmanesh, H.; Beves, J. E. Photosubstitution reactions in ruthenium(II) trisdiimine complexes: Implications for photoredox catalysis. *Polyhedron* **2019**, *160*, 1–9.
- (32) La Porte, N. T.; Martinez, J. F.; Chaudhuri, S.; Hedström, S.; Batista, V. S.; Wasielewski, M. R. Photoexcited radical anion super-reductants for solar fuels catalysis. *Coord. Chem. Rev.* **2018**, *361*, 98–119.

(33) Ghosh, I.; Ghosh, T.; Bardagi, J. I.; König, B. Reduction of aryl halides by consecutive visible light-induced electron transfer processes. *Science* **2014**, *346*, 725–728.

(34) MacKenzie, I. A.; Wang, L.; Onuska, N. P. R.; Williams, O. F.; Begam, K.; Moran, A. M.; Dunietz, B. D.; Nicewicz, D. A. Discovery and characterization of an acridine radical photoreductant. *Nature* **2020**, *580*, 76–80.

(35) Xu, J.; Cao, J.; Wu, X.; Wang, H.; Yang, X.; Tang, X.; Toh, R. W.; Zhou, R.; Yeow, E. K. L.; Wu, J. Unveiling Extreme Photoreduction Potentials of Donor–Acceptor Cyanoarenes to Access Aryl Radicals from Aryl Chlorides. *J. Am. Chem. Soc.* **2021**, *143*, 13266–13273.

(36) Jeong, D. Y.; Lee, D. S.; Lee, H. L.; Nah, S.; Lee, J. Y.; Cho, E. J.; You, Y. Evidence and Governing Factors of the Radical-Ion Photoredox Catalysis. *ACS Catal.* **2022**, *6047–6059*.

(37) Cole, J. P.; Chen, D.-F.; Kudisch, M.; Pearson, R. M.; Lim, C.-H.; Miyake, G. M. Organocatalyzed Birch Reduction Driven by Visible Light. *J. Am. Chem. Soc.* **2020**, *142*, 13573–13581.

(38) Targas, K.; Williams, O. P.; Wickens, Z. K. Unveiling Potent Photooxidation Behavior of Catalytic Photoreductants. *J. Am. Chem. Soc.* **2021**, *143*, 4125–4132.

(39) Wu, S.; Žurauskas, J.; Domański, M.; Hitzfeld, P. S.; Butera, V.; Scott, D. J.; Rehbein, J.; Kumar, A.; Thyrhaug, E.; Hauer, J.; Barham, J. P. Hole-mediated photoredox catalysis: tris(p-substituted)-biarylaminium radical cations as tunable, precomplexing and potent photooxidants. *Org. Chem. Front.* **2021**, *8*, 1132–1142.

(40) Rombach, D.; Wagenknecht, H.-A. Photoredox Catalytic α -Alkoxy pentafluorosulfanylation of α -Methyl- and α -Phenylstyrene Using SF₆. *Angew. Chem., Int. Ed.* **2020**, *59*, 300–303.

(41) Biesczad, B.; Karl, T. A.; Rolka, A. B.; Nuernberger, P.; Kutta, R. J.; König, B.; Oxidative con-PET Catalysis for Arene Functionalization. **2022. Catalysis**, DOI: 10.26434/chemrxiv-2022-39x5l. (accessed 2022-07-28).

(42) Moutet, J.-C.; Reverdy, G. Photochemistry of cation radicals in solution: photoinduced oxidation by the phenothiazine cation radical. *Tetrahedron Lett.* **1979**, *20*, 2389–2392.

(43) Christensen, J. A.; Phelan, B. T.; Chaudhuri, S.; Acharya, A.; Batista, V. S.; Wasielewski, M. R. Phenothiazine Radical Cation Excited States as Super-oxidants for Energy-Demanding Reactions. *J. Am. Chem. Soc.* **2018**, *140*, 5290–5299.

(44) Stockmann, A.; Kurzawa, J.; Fritz, N.; Acar, N.; Schneider, S.; Daub, J.; Engl, R.; Clark, T. Conformational control of photoinduced charge separation within phenothiazine–pyrene dyads. *J. Phys. Chem. A* **2002**, *106*, 7958–7970.

(45) Alkaitis, S. A.; Beck, G.; Graetzel, M. Laser photoionization of phenothiazine in alcoholic and aqueous micellar solution. Electron transfer from triplet states to metal ion acceptors. *J. Am. Chem. Soc.* **1975**, *97*, 5723–5729.

(46) Bandlish, B. K.; Padilla, A. G.; Shine, H. J. Ion radicals. XXXIII. Reactions of 10-methyl- and 10-phenylphenothiazine cation radicals with ammonia and amines. Preparation and reactions of 5-(N-alkyl)sulfilimines and 5-(N,N-dialkylamino)sulfonium salts. *J. Org. Chem.* **1975**, *40*, 2590–2595.

(47) Jia, P.; Li, Q.; Poh, W. C.; Jiang, H.; Liu, H.; Deng, H.; Wu, J. Light-Promoted Bromine-Radical-Mediated Selective Alkylation and Amination of Unactivated C(sp³)–H Bonds. *Chem* **2020**, *6*, 1766–1776.

(48) Wu, Y.; Xu, S.; Wang, H.; Shao, D.; Qi, Q.; Lu, Y.; Ma, L.; Zhou, J.; Hu, W.; Gao, W.; Chen, J. Directing Group Enables Electrochemical Selectively Meta-Bromination of Pyridines under Mild Conditions. *J. Org. Chem.* **2021**, *86*, 16144–16150.

(49) Wolfenden, B. S.; Willson, R. L. Radical-cations as reference chromogens in kinetic studies of one-electron transfer reactions: pulse radiolysis studies of 2,2'-azinobis-(3-ethylbenzthiazoline-6-sulphonate). *J. Chem. Soc., Perkin Trans. 2* **1982**, *2*, 805–812.

(50) Bard, A. J.; Ledwith, A.; Shine, H. J. Formation, Properties and Reactions of Cation Radicals in Solution. In *Advances in Physical Organic Chemistry*, Gold, V.; Bethell, D., Eds.; Academic Press: 1976; *13*, 155–278.

(51) Anbar, M.; Thomas, J. K. Pulse Radiolysis Studies of Aqueous Sodium Chloride Solutions I. *J. Phys. Chem.* **1964**, *68*, 3829–3835.

(52) Buxton, G. V.; Bydder, M.; Arthur Salmon, G. Reactivity of chlorine atoms in aqueous solution Part 1 The equilibrium Cl⁺–Cl=Cl₂. *J. Chem. Soc., Faraday Trans.* **1998**, *94*, 653–657.



CAS BIOFINDER DISCOVERY PLATFORM™

PRECISION DATA FOR FASTER DRUG DISCOVERY

CAS BioFinder helps you identify targets, biomarkers, and pathways

Unlock insights

CAS
A division of the American Chemical Society